Behaviour of the numerical entropy production of the one-and-a-half-dimensional shallow water equations

Sudi Mungkasi[1] Stephen G. Roberts[2]

(Received 18 October 2012; revised 19 March 2013)

Abstract

This article reports the behaviour of the numerical entropy production of the one-and-a-half-dimensional shallow water equations. The one-and-a-half-dimensional shallow water equations are the one-dimensional shallow water equations with a passive tracer or transverse velocity. The studied behaviour is with respect to the choice of numerical fluxes to evolve the mass, momentum, tracer-mass (transverse momentum), and entropy. When solving the one-and-a-half-dimensional shallow water equations using a finite volume method, we recommend the use of a double sided stencil flux for the mass and momentum, and in addition, a single sided stencil (upwind) flux for the tracer-mass. Having this recommended combination of fluxes, we use a double sided

http://journal.austms.org.au/ojs/index.php/ANZIAMJ/article/view/6243
 Published May 5, 2013, as part of the Proceedings of the 16th Biennial Computational Techniques and Applications Conference. ISSN 1446-8735. (Print two pages per sheet of paper.)

stencil entropy flux to compute the numerical entropy production, but this flux generates positive overshoots of the numerical entropy production. Positive overshoots of the numerical entropy production are avoided by use of a modified entropy flux, which satisfies a discrete numerical entropy inequality.
Subject class: 65M08, 65M50, 76M12
Keywords: numerical entropy production, smoothness indicator, refinement indicator, finite volume methods, shallow water equations, passive tracer, transverse velocity

Contents

1 Introduction

A hyperbolic system of conservation laws satisfies an entropy inequality. Entropy is a quantity defined based on the conserved quantities. For smooth solutions, the entropy inequality becomes an equation: the entropy equation. For nonsmooth solutions, the entropy inequality becomes a strict inequality. Evolving the entropy numerically leads to a computational error. The local

truncation error of the entropy is called the numerical entropy production (NEP).

The NEP indicates the smoothness of solutions to hyperbolic systems of conservation laws [4]. One example of conservation laws is the system of one-and-a-half dimensional shallow water equations (1.5D SWE). The 1.5D SWE are the one-dimensional shallow water equations (1D SWE) with a passive tracer or transverse velocity. The conserved quantities of the 1D SWE are the mass and momentum. Therefore, the conserved quantities of the 1.5D SWE are the mass, momentum, and tracer-mass (transverse momentum). The 1.5D SWE admit discontinuous solutions, namely shock and contact discontinuities [2]. The NEP indicator detects these discontinuities by producing larger values of indicators than the values on smooth regions.

By definition, an entropy production is nonpositive. Nevertheless, Puppo and Semplice [4] proved that positive overshoots of the NEP were possible when conservation laws were solved using a finite volume method with the same type of numerical fluxes for the evolutions of all conserved quantities. The numerical flux used by Puppo and Semplice [4] was the Lax–Friedrichs flux, which is a double sided stencil flux. In their work, shallow water equations were not particularly considered.

With a finite volume method to solve the 1.5D SWE, we could use the same type of numerical fluxes having a double sided stencil formulation. However, to get a more accurate solution to the passive tracer or transverse velocity, the strategy is as follows: for the evolutions of conserved quantities of the 1D SWE we use the same type of numerical fluxes having double sided stencil formulations, but for the evolution of the tracer-mass we use the upwind numerical flux (single- sided stencil flux), as suggested by Bouchut [1]. The choice of numerical flux functions to solve the governing equations affects the accuracy of the numerical solutions. Furthermore, the choice of numerical flux functions to solve the governing equations and to evolve the entropy affect the behaviour of the NEP.

The goal of this article is to report the behaviour of the NEP with respect

to several combinations of numerical fluxes. With a finite volume method, the numerical fluxes are used to evolve the mass, momentum, tracer-mass (transverse momentum), and entropy for the 1.5D SWE.

2 Governing equations and the numerical entropy production

We present the 1.5D SWE and how we compute the NEP. In the 1.5D SWE, the dynamics of the passive tracer is governed by an additional transport (advection) equation to the 1D SWE. This additional transport equation does not influence the fluid dynamics of the 1D SWE. Note that the concentration of the passive tracer in the passive tracer framework is in place of the transverse velocity in the transverse velocity framework.

We limit our discussion to shallow water flows on a horizontal topography (without source terms). The 1.5D SWE are

$$h_t + (hu)_x = 0\,, \tag{1}$$

$$(hu)_t + \left(hu^2 + \frac{1}{2}gh^2\right)_x = 0\,, \tag{2}$$

$$(hv)_t + (huv)_x = 0\,. \tag{3}$$

Here, x represents the coordinate in one-dimensional space, t represents the time variable, g is the acceleration due to gravity, $h = h(x,t)$ denotes the water height, $u = u(x,t)$ denotes the water velocity in the x-direction, and $v(x,t)$ is the transverse velocity or the concentration of the passive tracer. The transverse velocity is orthogonal to the x-axis and has a horizontal direction. The conserved quantities of the 1.5D SWE are the mass or water height h, momentum hu, and tracer-mass or transverse momentum hv. Our discussion does not include bed drag or viscous or turbulent dissipation.

The entropy inequality for (1)–(3) is

$$\eta_t + \psi_x \leqslant 0\,, \tag{4}$$

where the entropy (the physical energy) η and the entropy flux (the flux of the physical energy) ψ are

$$\eta\left(\mathbf{q}(x,t)\right) = \frac{1}{2}h(u^2+v^2) + \frac{1}{2}gh^2\,, \tag{5}$$

$$\psi\left(\mathbf{q}(x,t)\right) = \left[\frac{1}{2}h(u^2+v^2) + gh^2\right]u\,, \tag{6}$$

and $\mathbf{q}(x,t) = (h\ hu\ hv)^T$ is the vector of conserved quantities of the 1.5D SWE. Inequality (4) is to be understood in the weak sense. For smooth solutions, inequality (4) becomes an equation and is called the entropy equation. For nonsmooth solutions, it becomes a strict inequality. Inequality (4) is described in further detail by Bouchut [1], amongst others.

We adapt the existing numerical entropy scheme described in our previous work [3]. The numerical entropy production (NEP) in the jth cell at the nth time step is

$$E_j^n = \frac{1}{\Delta t}\left[\eta\left(\mathbf{Q}_j^n\right) - \Theta_j^n\right], \tag{7}$$

which is the local truncation error of the entropy at the corresponding cell and the corresponding time. Here, Θ_j^n is an approximation of the average of the exact entropy η in the jth cell at the nth time step and calculated using the numerical entropy scheme with $\eta\left(\mathbf{Q}^{n-1}\right)$ as the input, $\mathbf{Q}_j^n$ is an approximation of the average of the exact quantity $q_j\left(x,t^n\right)$ in the jth cell at the nth time step ($t = t^n$) and calculated using the numerical conserved quantity scheme with $\mathbf{Q}^{n-1}$ as the input, and Δt is the time step used in both numerical schemes.

3 Flux functions for finite volume methods

This section provides three combinations of numerical flux functions for finite volume methods used to solve the 1.5D SWE.

Conservation laws

$$q_t + f(q)_x = 0 \tag{8}$$

are solved using a first order finite volume method [2]

$$Q_j^{n+1} = Q_j^n - \lambda \left(F_{j+\frac{1}{2}}^n - F_{j-\frac{1}{2}}^n \right) . \tag{9}$$

Here $F_{j+\frac{1}{2}}$ and $F_{j-\frac{1}{2}}$ are numerical fluxes of the conserved quantities computed in such a way that the method is stable with $\lambda = \Delta t/\Delta x$. Variables Δt and Δx are the time step and cell-width. We assume that the spatial domain is discretised uniformly into a finite number of cells. The notation Q_j^n represents an approximation of the average of the exact quantity $q_j(x, t^n)$ in the jth cell at the nth time step. In addition, f is the analytical flux function.

For our numerical experiments on the 1.5D SWE, we consider a double sided stencil flux function and a single sided stencil flux function. In particular, we take the local Lax–Friedrichs flux and the upwind flux functions for numerical evolutions. As a double sided stencil flux, the local Lax–Friedrichs flux function is suitable for the evolution of all quantities (mass, momentum, tracer-mass, and entropy). As a single sided stencil flux, the upwind flux function is suitable for the evolution of the tracer-mass.

We consider three combinations of flux functions in our numerical schemes, namely:

A *local Lax–Friedrichs* flux for the mass, momentum, tracer-mass, and entropy evolutions;

B *local Lax–Friedrichs* flux for the mass, momentum, and entropy evolutions, *upwind* flux for the tracer-mass evolution; and

C *local Lax–Friedrichs* flux for the mass and momentum evolutions, *upwind* flux for the tracer-mass evolution, *modified* flux for the entropy evolution.

For our reference, we call these combinations of flux functions *Combination A*, *Combination B*, and *Combination C*, respectively.

In the evolution of the numerical conserved quantity scheme and the numerical entropy scheme, we can simply use the same type of flux function (in particular the local Lax–Friedrichs flux as we mentioned above) for evolving the mass, momentum, tracer-mass, and entropy. This motivates Combination A.

The local Lax–Friedrichs fluxes used for Combination A are described as follows. Consider the jth cell, which is the interval $(x_{j-\frac{1}{2}}, x_{j+\frac{1}{2}})$ of the uniformly discretised spatial domain. The local Lax–Friedrichs flux for the quantity evolution has the form [2, 4]

$$F^n_{j+\frac{1}{2}} = F(Q^n_{j+1}, Q^n_j) = \frac{1}{2}\left[f\left(Q^n_{j+1}\right) + f\left(Q^n_j\right) - \alpha^n_{j+\frac{1}{2}}\left(Q^n_{j+1} - Q^n_j\right)\right] \tag{10}$$

where $\alpha^n_{j+\frac{1}{2}} = \max\left(|u^n_{j+1}| + \sqrt{gh^n_{j+1}},\ |u^n_j| + \sqrt{gh^n_j}\right)$ is the coefficient of artificial diffusion, chosen at each time step locally. Notations u^n_j and h^n_j represent the numerical velocity and water height, respectively, in the jth cell at the nth time step. Recall that Q^n_j is an approximation of the average of the exact quantity $q_j(x, t^n)$ in the jth cell at the nth time step. The notation q, or q_j for the specific jth cell, represents the mass, momentum, or tracer-mass. Furthermore, the local Lax–Friedrichs flux for the entropy evolution is

$$\Psi^n_{j+\frac{1}{2}} = \Psi(\mathbf{Q}^n_{j+1}, \mathbf{Q}^n_j) = \frac{1}{2}\left\{\psi\left(\mathbf{Q}^n_{j+1}\right) + \psi\left(\mathbf{Q}^n_j\right) - \alpha^n_{j+\frac{1}{2}}\left[\eta\left(\mathbf{Q}^n_{j+1}\right) - \eta\left(\mathbf{Q}^n_j\right)\right]\right\} \tag{11}$$

where $\mathbf{Q}^n_j$ is an approximation of the average of the exact conserved quantity $\mathbf{q}_j(x, t^n)$ in the jth cell at the nth time step. To make the notation clear, we note that $\mathbf{Q}^n_j = [h^n_j\ (hu)^n_j\ (hv)^n_j]^\top$, where h^n_j is an approximation of the average of water height h in the jth cell at the nth time step. The notations $(hu)^n_j$ and $(hv)^n_j$ are understood similarly.

To get a more accurate solution of the tracer, a natural way is by using the upwind flux function for the evolution of the tracer-mass [1]. This leads to Combination B: the local Lax– Friedrichs flux for the mass, momentum, and entropy; and the upwind flux for the tracer-mass. For Combination B, the local Lax–Friedrichs flux for the mass and momentum is defined by (10). The local Lax–Friedrichs flux for the entropy is defined by (11). The upwind flux $F^{n,hv}_{j+\frac{1}{2}}$ for the tracer-mass at the spatial point $x = x_{j+\frac{1}{2}}$ at time $t = t^n$ is

$$F^{n,hv}_{j+\frac{1}{2}} = \begin{cases} F^{n,h}_{j+\frac{1}{2}} v_j & \text{if } F^{n,h}_{j+\frac{1}{2}} \geqslant 0\,, \\ F^{n,h}_{j+\frac{1}{2}} v_{j+1} & \text{otherwise}\,. \end{cases} \tag{12}$$

Here $F^{n,h}_{j+\frac{1}{2}}$ is the mass flux computed using the local Lax–Friedrichs flux (10) at the spatial point $x = x_{j+\frac{1}{2}}$ at time $t = t^n$.

In our numerical results presented in the next section (Section 4), we see that Combination B leads to positive overshoots of the NEP. To avoid positive overshoots of the NEP, the entropy flux is modified with respect to the local Lax–Friedrichs and upwind flux functions, because these two fluxes are used in the numerical conserved quantity scheme. With a particular modification of the entropy flux, the entropy evolutions satisfy a discrete numerical entropy inequality as described by Bouchut [1]. This leads to Combination C: the local Lax–Friedrichs flux for the mass and momentum, the upwind flux for the tracer-mass, and the modified flux for the entropy. For Combination C, the local Lax–Friedrichs flux for the mass and momentum is defined by (10). The upwind flux for the tracer-mass is defined by (12). The modified flux for the entropy is

$$\Psi^n_{j+\frac{1}{2}} = \Psi^{n,1d}_{j+\frac{1}{2}} + \Psi^{n,hv}_{j+\frac{1}{2}}\,. \tag{13}$$

Here, $\Psi^{n,1d}_{j+\frac{1}{2}}$ is a numerical entropy flux of the 1D SWE part at the nth time step. In our case $\Psi^{n,1d}_{j+\frac{1}{2}}$ is computed using the Lax–Friedrichs entropy flux, that is, the numerical entropy flux of the form (11) with setting $v = 0$. In addition, $\Psi^{n,hv}_{j+\frac{1}{2}}$ is a numerical entropy flux of the tracer part. In our case

$\Psi^{n,hv}_{j+\frac{1}{2}}$ is computed using the upwind entropy flux

$$\Psi^{n,hv}_{j+\frac{1}{2}} = \begin{cases} \frac{1}{2}F^{n,h}_{j+\frac{1}{2}}v^2_j & \text{if } F^{n,h}_{j+\frac{1}{2}} \geqslant 0\,, \\ \frac{1}{2}F^{n,h}_{j+\frac{1}{2}}v^2_{j+1} & \text{otherwise}\,. \end{cases} \tag{14}$$

This modified numerical entropy flux is adapted from Bouchut [1, equation (3.88) for more detail].

4 Numerical experiments

This section presents numerical results relating to the behaviour of the NEP of the 1.5D SWE. The three combinations, A, B and C, of flux functions are tested.

For our experiments, the numerical setting is as follows. First order methods are implemented. All variables are quantified in SI units. The acceleration due to gravity is taken as $g = 9.81$. The Courant–Friedrichs–Lewy number is 1.0. The discrete L^1 relative error

$$\mathcal{E}^{L^1}_Q = \frac{\sum_{j=1}^{N} \left| q(x_j, t^n) - Q^n_j \right|}{\sum_{j=1}^{N} |q(x_j, t^n)|} \tag{15}$$

is used to quantify numerical errors, where N is the number of cells, $q(x_j, t^n)$ is the exact quantity at $(x, t) = (x_j, t^n)$, and Q^n_j is an approximation of the average of the exact quantity $q_j(x, t^n)$ in the jth cell at the nth time step. The term "quantity" in this case represents the water mass (height) h, momentum hu, transverse momentum (tracer-mass) hv, velocity u, and transverse velocity (the concentration of the passive tracer) v. Note that the notation $q(x_j, t^n)$ is different from $q_j(x, t^n)$.

As the benchmark test case, we set up a dam break problem with a passive tracer as follows. A horizontal topography on the interval $[-2000, 2000]$ is

considered. The initial condition is

$$u(x,0) = 0\,, \tag{16}$$

$$v(x,0) = \begin{cases} 3 & \text{if } -2000 < x < 0\,, \\ 0 & \text{if } 0 < x < 2000\,, \end{cases} \tag{17}$$

$$h(x,0) = \begin{cases} 10 & \text{if } -2000 < x < 0\,, \\ 4 & \text{if } 0 < x < 2000\,. \end{cases} \tag{18}$$

This initial water height $h(x,0)$ is chosen in such a way that we clearly see a rarefaction, a contact discontinuity (a discontinuity between two different concentrations of the passive tracer), and a shock wave propagate at time $t > 0$. We could take a much smaller initial water height for $0 < x < 2000$, but the contact discontinuity and the shock wave would not be clearly seen, because the rarefaction would dominate the water motion at time $t > 0$. The exact analytical solution of the dam break problem was derived by Stoker [5]. LeVeque [2] reviewed shallow flows with a passive tracer. .

A comparison of numerical errors is given in Table 1. From Table 1, Combinations A, B and C lead to exactly the same results (and hence the same errors) in h and u. Combinations B and C lead to exactly the same results in v, while Combination A leads to larger errors of v than the errors of v produced by Combinations B and C. As the cells are uniformly refined, the errors get smaller and the numerical solutions better approximate the exact solution. Even though we use first order methods, the convergence is not of order of one, but less than one. This convergence is due to discontinuities occurring in the numerical solutions. We summarise in Table 1, Combinations B and C generate more accurate results and they have the same performance.

Some simulation results using Combinations A, B and C are illustrated in Figures 1, 2 and 3, respectively. In Figure 1, the numerical solution approximates the exact water surface (stage) and the exact velocity quite well. However, large errors occur around the contact discontinuity of the concentration $v(x,t)$ of the tracer. There are no positive overshoots of the

Table 1: Errors of $\mathfrak{h}$, $\mathfrak{u}$ and ν resulting from a finite volume method with fluxes using Combinations A, B and C for various numbers of cells. The errors are quantified at $\mathfrak{t} = 100$.

number of cells	$\mathfrak{h}$ error A, B, C	$\mathfrak{u}$ error A, B, C	ν error A	ν error B, C
100	0.019	0.108	0.070	0.037
200	0.012	0.066	0.050	0.026
400	0.007	0.038	0.035	0.019
800	0.004	0.022	0.025	0.013
1600	0.002	0.013	0.018	0.009

NEP in Figure 1. We restate that Combinations A and B lead to the same results in $\mathfrak{h}$ and $\mathfrak{u}$, but Combination B gives more accurate results in ν (see Table 1). However, Combination B produces positive overshoots and an oscillation of the NEP around the contact discontinuity, as shown in Figure 2. Furthermore, Combinations B and C produce the same errors in $\mathfrak{h}$, $\mathfrak{u}$ and ν, but no positive overshoots of the NEP are generated by Combination C as shown in Figure 3. In addition, Figure 2 suggests that Combination B results in a solution which does not satisfy a discrete entropy inequality, whereas Figures 1 and 3 suggest that Combinations A and C result in solutions which satisfy a discrete entropy inequality.

5 Conclusions

The use of a double sided stencil flux for the mass and momentum together with a single sided stencil (upwind) flux for the tracer-mass results in a more accurate solution than the solution produced by the use of the double sided stencil flux for all conserved quantity. This combination (double sided stencil flux for the mass and momentum, and upwind flux for the tracer-mass)

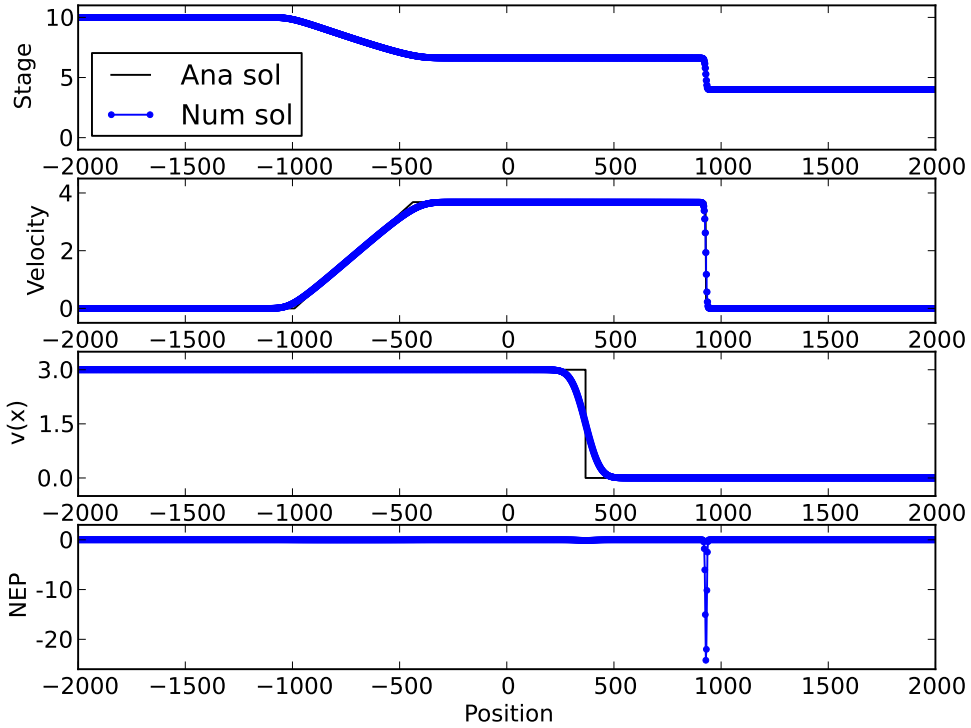

Figure 1: Results of a simulation using Combination A with 1600 cells at time $t = 100$. The NEP (7) is nonpositive everywhere. "Ana sol" and "Num sol" stand for analytical solution and numerical solution, respectively.

is recommended for solving the one- and-a-half dimensional shallow water equations in general. Note that the dam break problem with a passive tracer simulated is only an example to show the validity of our recommendation. The recommended combination of fluxes may or may not generate positive overshoots of the numerical entropy production, depending on the numerical flux function used in the entropy evolution. With the recommended combination, if we use the double sided stencil flux for the entropy, then we have positive overshoots and an oscillation of the numerical entropy production

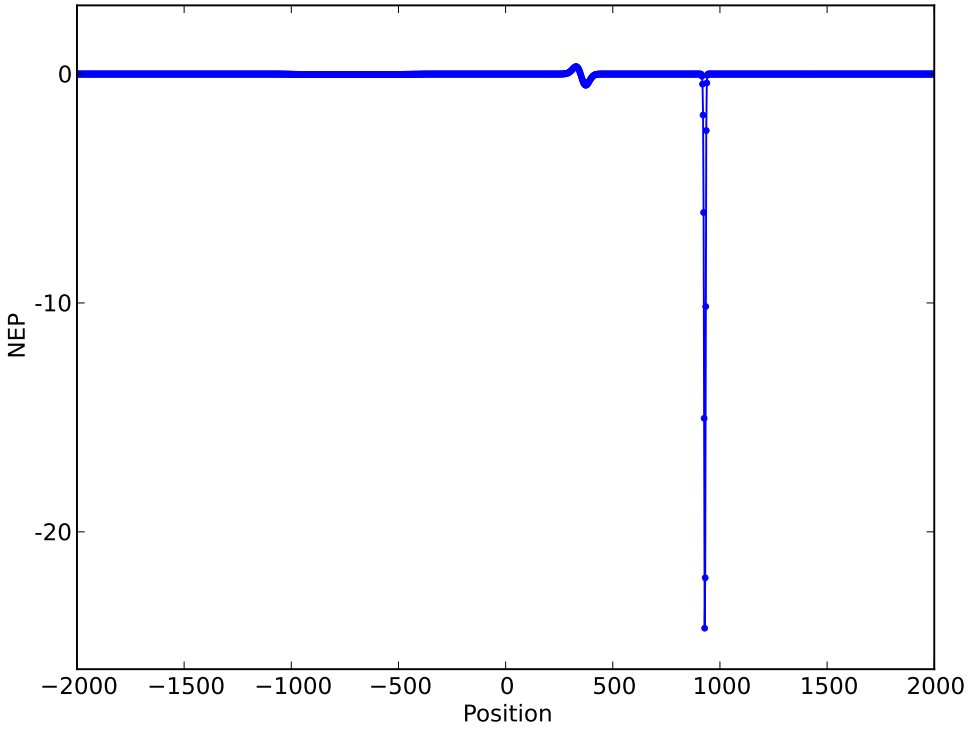

Figure 2: The NEP (7) resulting from Combination B with 1600 cells at $t = 100$. Positive overshoots of the NEP are generated around the contact discontinuity.

around a contact discontinuity. If we use a flux modified in such a way that a discrete numerical entropy inequality is satisfied, then no positive overshoots of the numerical entropy production are produced.

Positive overshoots and an oscillation of the numerical entropy production around a contact discontinuity are not completely bad. It is well-known that discontinuous solutions are difficult to resolve. Moreover, a contact discontinuity is much more difficult to resolve than a shock [4], and this is shown in our numerical experiments. When the numerical entropy production

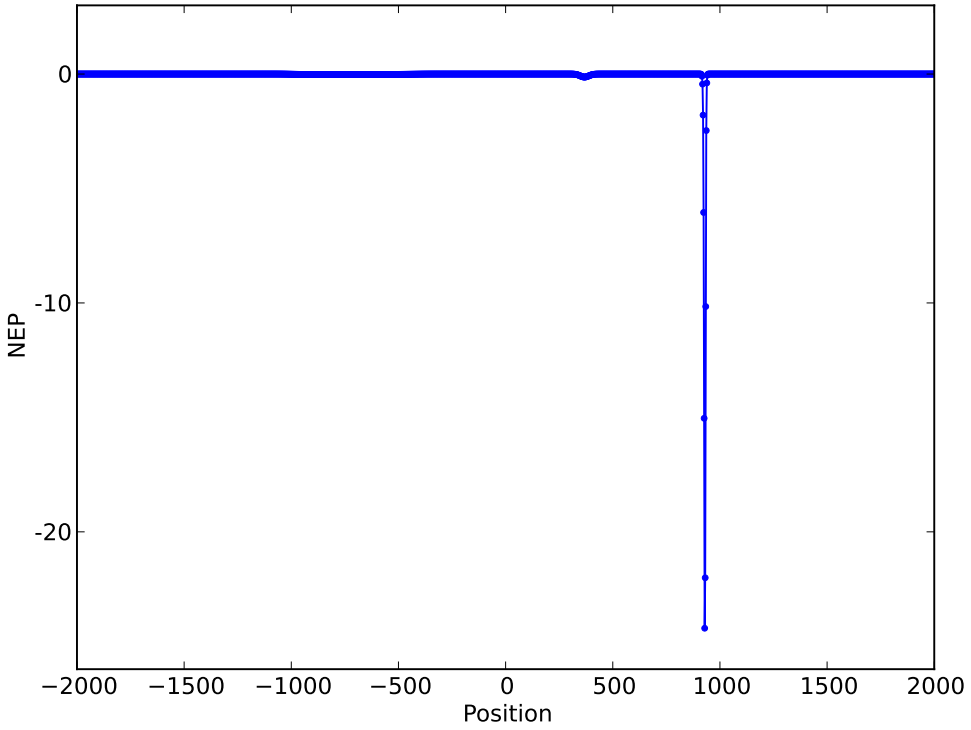

Figure 3: The NEP (7) resulting from Combination C with 1600 cells at $t = 100$. The NEP is nonpositive everywhere.

is implemented in an adaptive-mesh finite volume method as the refinement (smoothness) indicator, these positive overshoots and the oscillation of numerical entropy production might help in maintaining mesh refinement around the contact discontinuity. This maintenance in refinement is because, for the entropy around the contact discontinuity, the positive overshoots and the oscillation of the numerical entropy production are larger in magnitude than the numerical entropy production without positive overshoots produced by the modified flux.

Acknowledgements The work of Sudi Mungkasi was financially supported by The Australian National University. We thank Professor Sebastian Noelle of *Institut für Geometrie und Praktische Mathematik*, RWTH Aachen University, Germany for some discussions, and Professor Randall John LeVeque of the Department of Applied Mathematics, the University of Washington, USA for some comments.

References

[1] F. Bouchut. Efficient numerical finite volume schemes for shallow water models. In V. Zeitlin (editor), *Nonlinear dynamics of rotating shallow water: methods and advances*, Volume 2 of Edited series on advances in nonlinear science and complexity, pages 189–256. Elsevier, Amsterdam, 2007. http://dx.doi.org/10.1016/S1574-6909(06)02004-1 C20, C22, C25, C26

[2] R. J. LeVeque. *Finite-volume methods for hyperbolic problems*. Cambridge University Press, Cambridge, 2002. http://dx.doi.org/10.1017/CBO9780511791253 C20, C23, C24, C27

[3] S. Mungkasi and S. G. Roberts. Numerical entropy production for shallow water flows. *ANZIAM Journal*, 52(CTAC2010):C1–C17, 2011. http://journal.austms.org.au/ojs/index.php/ANZIAMJ/article/view/3786/1410 C22

[4] G. Puppo and M. Semplice. Numerical entropy and adaptivity for finite volume schemes. *Communications in Computational Physics*, 10(5):1132–1160, 2011. http://dx.doi.org/10.4208/cicp.250909.210111a C20, C24, C30

[5] J. J. Stoker. *Water Waves: The Mathematical Theory with Application*. Interscience Publishers, New York, 1957.

http://onlinelibrary.wiley.com/book/10.1002/9781118033159
C27

Author addresses

1. **Sudi Mungkasi**, Mathematical Sciences Institute, The Australian National University, Canberra, Australia; Department of Mathematics, Sanata Dharma University, Yogyakarta, Indonesia.
mailto:sudi.mungkasi@anu.edu.au;sudi@usd.ac.id

2. **Stephen G. Roberts**, Mathematical Sciences Institute, The Australian National University, Canberra, Australia.
mailto:stephen.roberts@anu.edu.au